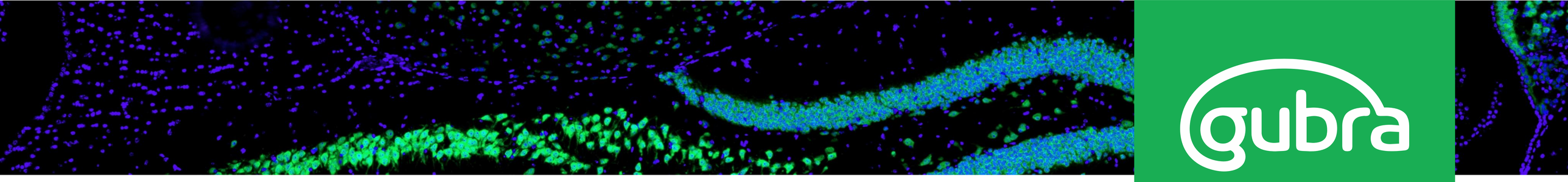

Quantitative whole-brain 3D imaging of dopaminergic cell architecture in the mouse MPTP model of Parkinson's disease

Authors
Henrik. H. Hansen, Urmas Roostalu, Casper Salinas, Jacob L. Skytte, Jacob Jelsing, Niels Vrang, Jacob Hecksher-Sørensen

Gubra, Hørsholm Kongevej 11B, Hørsholm, Denmark

Corresponding author
Henrik H. Hansen - hbh@gubra.dk

BACKGROUND & AIM

Parkinson's disease (PD) is a basal ganglia movement disorder characterized by progressive degeneration of the nigrostriatal dopaminergic system. The mouse MPTP model has for decades been the most widely used mouse model in preclinical drug development for PD. To date, histological studies in the MPTP mouse have largely focused on characterizing changes in preselected brain regions. To circumvent this limitation, we developed a combined light-sheet fluorescence microscopy (LSFM) and deep-learning pipeline to efficiently map and quantify changes in tyrosine hydroxylase-expressing neurocircuits at single-cell level throughout the intact brain of the MPTP mouse.

METHODS

Male C57BL/6JRj mice received four successive injections (IP, once every 2h) of vehicle (n=7) or MPTP (20 mg/kg, n=9). Brains were sampled at 7 days post-injection, immunostained for tyrosine hydroxylase (TH), cleared using iDISCO, and scanned on a light-sheet fluore-scence microscope. Deep-learning computational analysis was applied for automated segmentation, anatomical mapping, quantification of TH signal intensity and counting of total midbrain TH-positive neurons. For further details, see Roostalu *et al.* Disease Models & Mechanisms 12(11):dmm042200, 2019.

CONCLUSION

+ Combined LSFM-deep learning pipeline permits fully automated 3D mapping and quantification of TH-positive cells throughout the intact mouse brain
+ Quantitative 3D whole-brain imaging analysis reveals widespread and complex changes in central catecholaminergic neurocircuits in the MPTP mouse
+ The 3D imaging pipeline is advantageous for mapping and quantifying brain-wide effects of compounds targeting dopaminergic neurons in mouse models of Parkinson's disease

Explore **www.neuropedia.dk**
Gubra's open access resource of interactive mouse whole-brain histology maps

NeuroPedia

1 High-throughput whole-brain 3D imaging pipeline

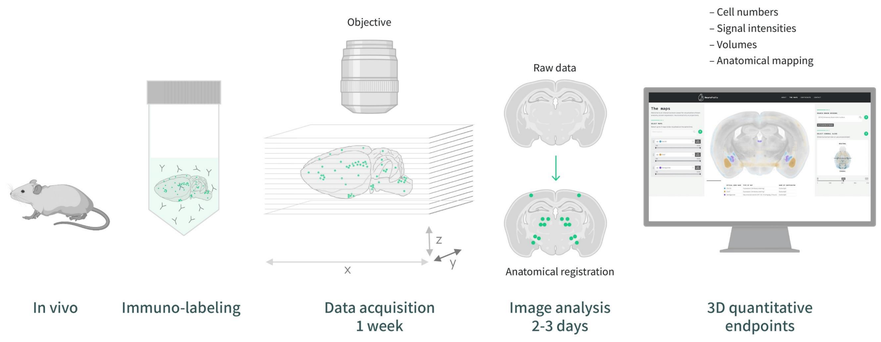

~6 weeks in total (≥30 brains per week)

2 Generation of brain-wide TH expression map

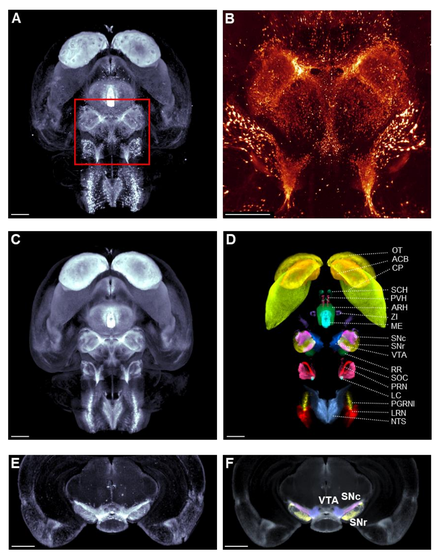

Figure 2. Brain-wide mapping of TH expression. **(A)** Light-sheet fluorescence brain imaging of TH expression in vehicle-dosed control mouse. **(B)** Further magnification (5×) of boxed midbrain area in panel A. **(C)** Mean fluorescence intensity map of TH expression (n=7 mice). **(D)** Average TH expression map in major catecholaminergic brain regions (color-coded for easier visualization). **(E,F)** Virtual cross-section through the midbrain, depicting TH expression in the ventral tegmental area (VTA, dark purple) and substantia nigra (SNc, pars compacta, light purple; SNr, pars reticulata, yellow). For other anatomical abbreviations, see list below. Scale bars: 1 mm.

3 Automated 3D counting of TH-positive neurons

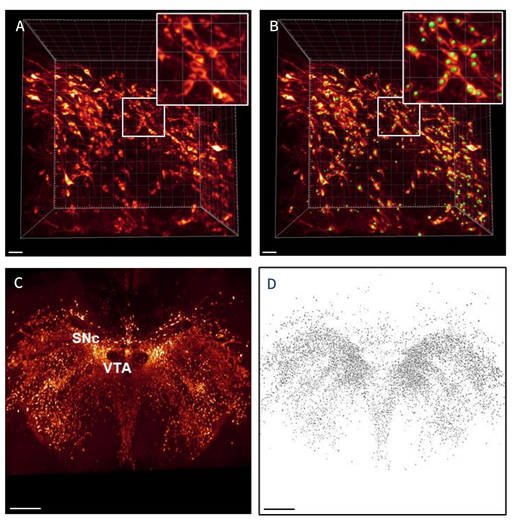

Figure 3. Deep learning-based total counting of TH-positive cells in the mouse midbrain. **(A)** Cell nuclei distinguishable in high-resolution scan of TH-stained mouse brain. **(B)** Deep-learning computational model enabling automated identification and registration of nuclei (green dots) in TH-expressing cells. Boxed area is magnified in upper right corner. **(C,D)** Automated detection of TH-positive cells in midbrain whole 3D-image stack from vehicle-dosed control mouse. Panel C, dorsal view; panel D, corresponding map of TH-positive cells detected in the sample. SNc, substantia nigra pars compacta; VTA, ventral tegmental area. Scale bars: 500 µm.

4 Whole-brain imaging analysis of TH signals in MPTP mice

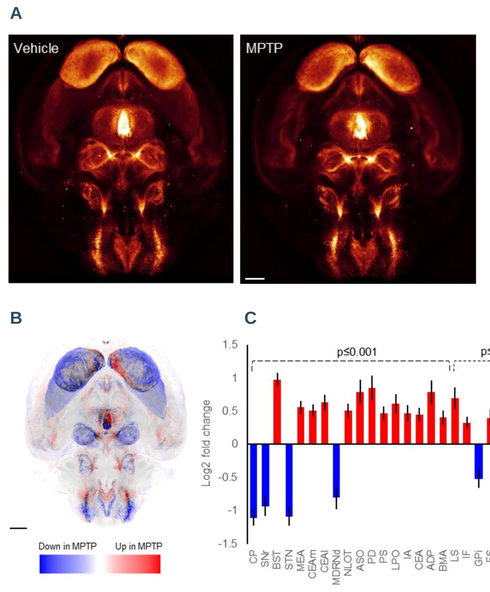

Fig. 4. Automated whole-brain imaging of MPTP-induced changes in TH expression. **(A)** Mean fluorescence intensity of TH expression in vehicle-dosed control mice (left panel, n=7) and MPTP mice (right panel, n=9). TH expression from each scanned brain was transferred to an average brain 3D coordinate mesh with mean expression calculated for each voxel. **(B)** Mean change in TH expression in MPTP-dosed mice relative to vehicle-dosed control mice. Brain regions with significantly altered average TH signal intensity are delineated in blue (downregulation) or red (upregulation). **(C)** Fold change (log2 scale) in TH expression of MPTP mice compared to vehicle controls. Only regions that show a statistically significant change between the groups are indicated. Scale bars: 1 mm. For anatomical abbreviations, see list below.

5 Voxel-based whole-brain quantitative analysis

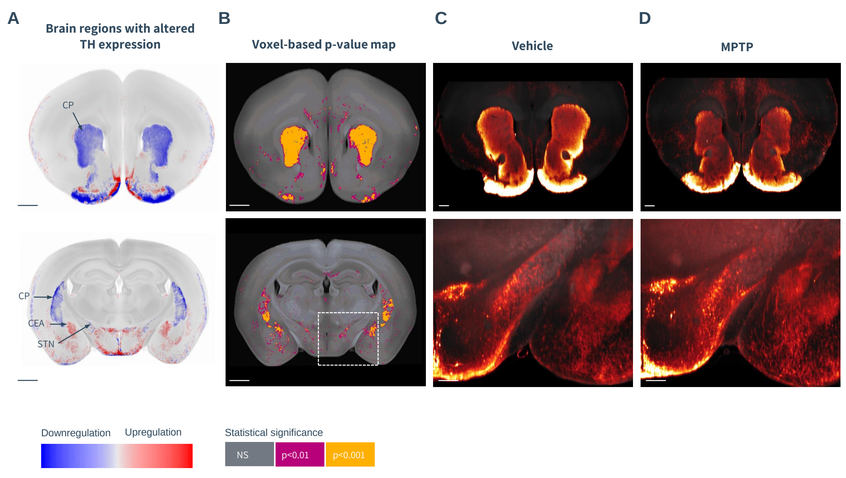

Figure 5. Automated voxel-based whole-brain quantitative analysis of changes in TH expression. **(A)** Virtual coronal sections (20 µm) from 3D-reconstructed average MPTP mouse brain. MPTP mouse brain regions with significantly altered mean TH signal intensity are delineated in blue (downregulation) or red (upregulation), as compared to vehicle controls. **(B)** Voxel-based statistical analysis. Brain regions in MPTP mice with significant regulation of TH expression are indicated, as compared to vehicle controls (P<0.01 and P<0.001; NS, non-significant). **(C, D)** Representative LSFM images from vehicle control and MPTP mouse, respectively. CEA, central amygdala nucleus; CP, caudate-putamen; STN, subthalamic nucleus. Scale bars: 1 mm in A,B; 500 µm in C,D.

6 3D counting of midbrain TH-positive neurons in MPTP mice

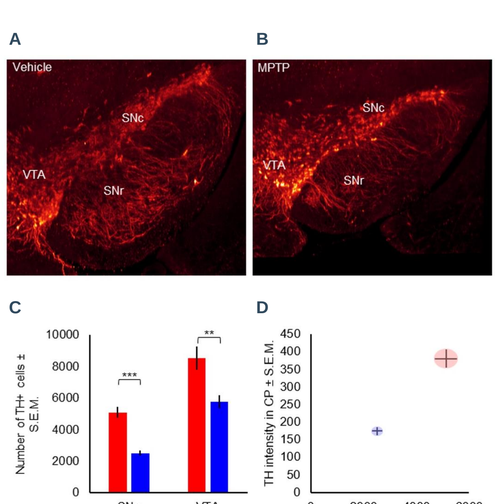

Fig. 6. (A,B) Coronal midbrain sections constructed from the whole 3D-image stack in representative vehicle- and MPTP-dosed mice, respectively. **(C)** Automated deep learning-based counting of TH-positive neurons in the SNc and VTA. **P<0.01; ***P<0.001 (one-way ANOVA, compared to vehicle controls). **(D)** TH signal intensity in the caudate–putamen plotted against corresponding number of TH-positive cells in the SNc. **(E)** Impaired motor coordination in MPTP mice, as analysed over three consecutive rotarod tests separated by 30 min (performed on study day 6) . *P<0.05; ***P<0.001 (two-way ANOVA, compared to vehicle controls). **(F)** Correlation of rotarod test performance vs. total number of TH-positive cells in the SNc.

Scan the QR code
to see 3D movie of TH-positive neuron distribution in the intact mouse brain

Anatomical abbrevations: **ACB**, nucleus accumbens; **ADP**, anterodorsal preoptic nucleus; **ARH**, arcuate nucleus; **ASO**, accessory supraoptic group; **BMA**, basomedial amygdalar nucleus; **BST**, bed nucleus of stria terminalis; **CP**, caudate–putamen; **CEA**, central amygdalar nucleus (CEAl+CEAm); **CEAl**, central amygdalar nucleus, lateral part; **CEAm**, central amygdalar nucleus (medial part); **DMH**, dorsomedial nucleus of the hypothalamus; **FS**, fundus of striatum; **GPi**, globus pallidus (internal segment); **IA**, intercalated amygdala nucleus; **IF**, interfascicular nucleus raphe; **LC**, locus coeruleus; **LGv**, lateral geniculate complex (ventral part); **LPO**, lateral preoptic area; **LRN**, lateral reticular nucleus; **LS**, lateral septal nucleus; **MDRNd**, medullary reticular nucleus (dorsal part); **ME**, median eminence; **MEA**, medial amygdala nucleus; **NLOT**, nucleus of the lateral olfactory tract; **NTS**, nucleus of the solitary tract; **OT**, olfactory tubercle; **PD**, posterodorsal preoptic nucleus; **PGRNl**, paragigantocellular nucleus; **PH**, posterior hypothalamic nucleus; **PRN**, pontine reticular formation; **PS**, parastrial nucleus; **PVH**, paraventricular nucleus; **RR**, retrorubral field; **SCH**, suprachiasmatic nucleus; **SNc**, substantia nigra pars compacta; **SNr**, substantia nigra pars reticulata; **SOC**, superior olivary complex; **VTA**, ventral tegmental area; **ZI**, zona incerta.

www.gubra.dk